

5

$U(1)$ and $SU(n)$ gauge theory

In this chapter we make a first exploration of $U(1)$ and $SU(n)$ ‘pure gauge theories’ (i.e. without electrons or quarks etc.), the static potential and the glueball masses.

5.1 Potential at weak coupling

According to (4.206) the static potential $V(r)$ in a gauge theory is given by the formula

$$V(r) = - \lim_{t \rightarrow \infty} \frac{1}{t} \ln W(r, t), \quad (5.1)$$

where $W(r, t)$ is a rectangular $r \times t$ Wilson loop in a lattice of infinite extent in the time direction (figure 5.1). We shall first evaluate this formula for free gauge fields and then give the results of the first non-trivial order in the weak-coupling expansion. This will illustrate that (5.1) indeed gives the familiar Coulomb potential plus corrections.

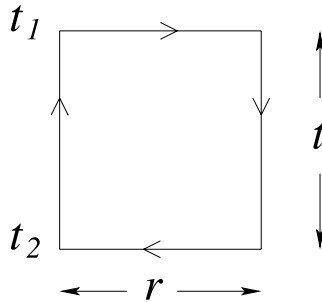


Fig. 5.1. A rectangular Wilson loop for the evaluation of the potential.

First we consider the compact $U(1)$ gauge theory (4.182), in which the external source $J_\mu(x)$ specified in (4.186) serves to introduce the Wilson loop. In this case (5.1) can be rewritten as

$$V(r) = - \lim_{t \rightarrow \infty} \frac{1}{t} \ln \left[\frac{Z(J)}{Z(0)} \right]. \tag{5.2}$$

The weak-coupling expansion can be obtained by substituting $U_\mu(x) = \exp[-igaA_\mu(x)]$ into the action,

$$S = - \sum_{x\mu\nu} \left(\frac{1}{4} [F_{\mu\nu x}]^2 - \frac{1}{48} g^2 a^2 [F_{\mu\nu x}]^4 + \dots \right), \tag{5.3}$$

$$F_{\mu\nu x} = \partial_\mu A_{\nu x} - \partial_\nu A_{\mu x}, \tag{5.4}$$

and expanding the path integral in the gauge coupling g . The first term in (5.3) is the usual free Maxwell action (non-compact $U(1)$ theory). The other terms are interaction terms special to the compact $U(1)$ theory.

As usual, gauge fixing is necessary in the weak-coupling expansion. This can be done on the lattice in the same way as in the continuum formulation. We shall not go into details here (cf. problem (i)), and just state that the free part of S (the part quadratic in A_μ) leads in the Feynman gauge to the propagator

$$\begin{aligned} D_{\mu\nu}(p) &= \delta_{\mu\nu} \frac{a^2}{\sum_\mu (2 - 2 \cos ap_\mu)}, \\ &= \delta_{\mu\nu} \frac{1}{p^2}, \quad ap \rightarrow 0. \end{aligned} \tag{5.5}$$

This is similar to the boson propagator (2.111). In position space

$$\begin{aligned} D_{\mu\nu}(x-y) &\equiv D_{xy}^{\mu\nu} = \delta_{\mu\nu} \int_{-\pi/a}^{\pi/a} \frac{d^4 p}{(2\pi)^4} e^{ip(x-y)} \frac{a^2}{\sum_\mu (2 - 2 \cos ap_\mu)} \\ &\rightarrow \delta_{\mu\nu} \frac{1}{4\pi^2(x-y)^2}, \quad (x-y)^2/a^2 \rightarrow \infty. \end{aligned} \tag{5.6}$$

The large- x behavior of $D_{\mu\nu}(x)$ corresponds to the small- p behavior of $D_{\mu\nu}(p)$. This can be shown with the help of the saddle-point method for evaluating the large- x behavior.

To leading order in g^2 , $Z(J)$ is given by

$$Z(J) = e^{\frac{1}{2} g^2 \sum_{xy} J_\mu(x) D_{\mu\nu}(x-y) J_\nu(y)} Z(0), \tag{5.7}$$

and

$$V(r) = - \frac{1}{t} \frac{1}{2} g^2 \sum_{xy} J_\mu(x) D_{\mu\nu}(x-y) J_\nu(y), \quad t \rightarrow \infty. \tag{5.8}$$

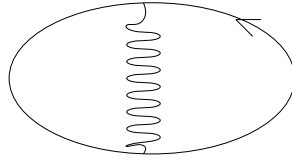


Fig. 5.2. Diagram illustrating $\frac{1}{2}g^2 \sum J D J$.

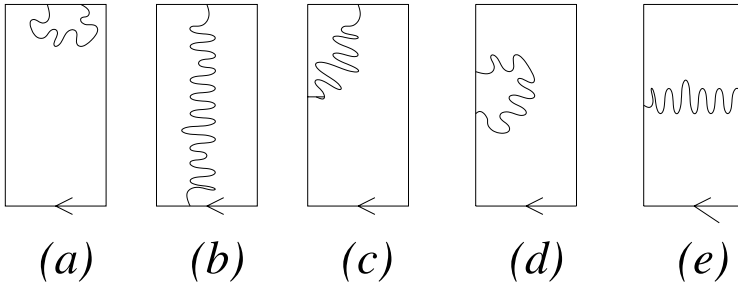


Fig. 5.3. Typical contributing diagrams.

This expression leads to the diagram in figure 5.2. With the currents J flowing according to figure 5.1, the following types of contributions can be distinguished (figure 5.3). Diagram (d) is a self-energy contribution,

$$\frac{1}{2}g^2 \sum_{(d)} J D J = \frac{1}{2}g^2(i)^2 \sum_{x_4, y_4 = -t/2}^{t/2} D_{44}(\mathbf{0}, x_4 - y_4), \quad (5.9)$$

where the times t_1 and t_2 in figure 5.1 have been taken as $\pm t/2$. We may first sum over y_4 . For $t \rightarrow \infty$ this summation converges at large y_4 and becomes independent of x_4 . The summation over y_4 sets p_4 in the Fourier representation for D to zero (cf. (2.90)),

$$\begin{aligned} \frac{1}{2}g^2 \sum_{(d)} J D J &\sim -\frac{1}{2}g^2 t \sum_{y_4 = -\infty}^{\infty} D_{44}(\mathbf{0}, x_4 - y_4) \\ &= -\frac{1}{2}g^2 t \int_{-\pi/a}^{\pi/a} \frac{d^4 p}{(2\pi)^4} e^{ip_4(x_4 - y_4)} \frac{a^2}{\sum_{\mu} (2 - 2 \cos ap_{\mu})} \\ &= -\frac{1}{2}g^2 t \int_{-\pi/a}^{\pi/a} \frac{d^3 p}{(2\pi)^3} \frac{a^2}{\sum_{j=1}^3 (2 - 2 \cos ap_j)} \\ &= -\frac{1}{2}g^2 t v(\mathbf{0}), \end{aligned} \quad (5.10)$$

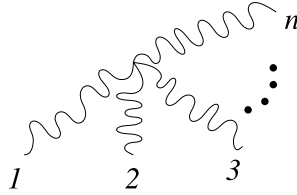


Fig. 5.4. Vertices in the compact $U(1)$ theory.

where

$$v(\mathbf{x}) = \int_{-\pi/a}^{\pi/a} \frac{d^3p}{(2\pi)^3} e^{i\mathbf{p}\mathbf{x}} \frac{a^2}{\sum_{j=1}^3 (2 - 2 \cos ap_j)} \tag{5.11}$$

is the lattice-regularized Coulomb potential. Its numerical value at the origin is given by

$$av(\mathbf{0}) = 0.253 \dots \tag{5.12}$$

The contribution of type (e) is given by

$$\frac{1}{2}g^2 \sum_{(e)} J D J \sim \frac{1}{2}g^2 i(-i) \int_{-t/2}^{t/2} dx_4 dy_4 \frac{1}{4\pi^2[(x_4 - y_4)^2 + r^2]}, \tag{5.13}$$

where we assumed $r/a \gg 1$ such that the asymptotic form (5.6) is valid and the summations over x_4 and y_4 may be replaced by integrations. Proceeding as for diagram (d) we get

$$\begin{aligned} \frac{1}{2}g^2 \sum_{(e)} J D J &\sim \frac{1}{2}g^2 t \int_{-\infty}^{\infty} dy_4 \frac{1}{4\pi^2[(x_4 - y_4)^2 + r^2]} \\ &= \frac{1}{2}g^2 t \frac{1}{4\pi r}. \end{aligned} \tag{5.14}$$

From these example calculations it is clear that the diagrams of types (a), (b) and (c) do not grow linearly with t . Remembering that there are two contributions of types (d) and (e) (related by interchanging x and y) we find for the potential to order g^2

$$V(\mathbf{x}) = g^2[v(\mathbf{0}) - v(\mathbf{x})], \tag{5.15}$$

as expected.

Let us now briefly consider higher-order corrections in the compact $U(1)$ theory. The series (5.3) for S leads to interaction vertices of the type shown in figure 5.4, which are proportional to $(ag)^{n-2}$. Their effect vanishes in the continuum limit, unless the powers of a are compensated

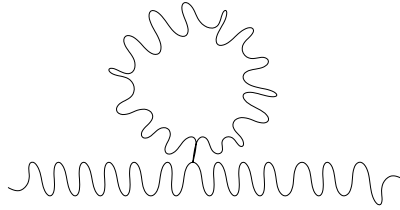


Fig. 5.5. A self-energy diagram in the compact $U(1)$ theory.

by powers of a^{-1} coming from divergent loop diagrams. An example of this is the self-energy diagram figure 5.5, which leads to a ‘vacuum-polarization tensor’ (cf. problem (ii))

$$\Pi_{\mu\nu}(p) = -\frac{1}{4}g^2(\delta_{\mu\nu}p^2 - p_\mu p_\nu) + O(a^2), \quad (5.16)$$

and a modified propagator

$$D'^{-1}_{\mu\nu} = p^2\delta_{\mu\nu} + O(a^2) + \Pi_{\mu\nu}(p), \quad (5.17)$$

$$D'_{\mu\nu}(p) = Z(g^2)\delta_{\mu\nu}\frac{1}{p^2} + \text{terms} \propto p_\mu p_\nu, \quad (5.18)$$

$$Z(g^2) = [1 - \frac{1}{4}g^2 + O(g^4)]^{-1}. \quad (5.19)$$

The terms $\propto p_\mu p_\nu$ do not contribute to the Wilson loop because of gauge invariance, as expressed by ‘current conservation’ $\partial'_\mu J_{\mu x} = 0$. Further analysis leads to the conclusion that there are no other effects of the self-interaction in the weak-coupling-expansion continuum limit. Note that $Z(g^2)$ is finite, i.e. it does not diverge as $a \rightarrow 0$.

We conclude that in the compact $U(1)$ theory the potential is given by

$$V(r) = -g^2 Z(g^2) \frac{1}{4\pi r} + \text{constant} + O(a^2), \rightarrow \infty, \quad (5.20)$$

which is just a Coulomb potential. To make contact with the free Maxwell theory we identify the fine-structure constant α ,

$$\alpha = \frac{e^2}{4\pi} = \frac{g^2 Z(g^2)}{4\pi}. \quad (5.21)$$

The compact $U(1)$ theory is equivalent to the free Maxwell field at weak coupling.

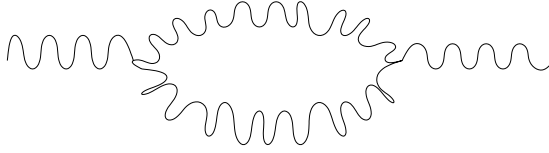


Fig. 5.6. Gluon self-energy contribution to the Wilson loop.

We now turn to the $SU(n)$ gauge theory. A calculation to order g^4 gives in this case the result for the magnitude of the force, $F(r)$, neglecting $O(a^2)$:

$$F(r) = \frac{\partial V(r)}{\partial r} = \frac{1}{4\pi r^2} C_2 \left\{ g^2 + \frac{11n}{48\pi^2} g^4 \left[\ln\left(\frac{r^2}{a^2}\right) + c \right] + O(g^6) \right\}. \quad (5.22)$$

Here C_2 is the value of the quadratic Casimir operator in the representation of the Wilson loop and c is a numerical constant which depends on lattice details. Some aspects of the calculation are described in [43]. The logarithm in (5.22) comes from the Feynman gauge self-energy contribution shown in figure 5.6, which is not present in the $U(1)$ theory. The formula (5.22) exhibits the typical divergencies occurring in perturbation theory. It diverges logarithmically as $a \rightarrow 0$. This problem is resolved by expressing physically measurable quantities in terms of each other. Here we shall choose an intuitive definition of a renormalized coupling constant g_R at some reference length scale d , by writing

$$F(d) = \frac{C_2 g_R^2}{4\pi d^2}. \quad (5.23)$$

This g_R is defined independently of perturbation theory. Its expansion in g^2 follows from (5.22),

$$g_R^2 = g^2 + \frac{11n}{48\pi^2} \left[\ln\left(\frac{d^2}{a^2}\right) + c \right] g^4 + \dots, \quad (5.24)$$

which may be inverted,

$$g^2 = g_R^2 - \frac{11n}{48\pi^2} \left[\ln\left(\frac{d^2}{a^2}\right) + c \right] g_R^4 + \dots. \quad (5.25)$$

The original parameter g in the action has to depend on a if we want to get a g_R independent of a . This dependence is here known incompletely: we cannot take the limit $a \rightarrow 0$ in (5.25) because then the coefficient of g_R^4 blows up (and similarly for the higher-order coefficients). The limit

$a \rightarrow 0$ will be discussed in the following sections. Insertion into (5.22) leads to the form

$$F(r) = \frac{1}{4\pi r^2} C_2 \left[g_R^2 + \frac{11n}{48\pi^2} g_R^4 \ln\left(\frac{r^2}{d^2}\right) + O(g_R^6) \right], \quad (5.26)$$

from which all dependence on a has disappeared to this order in g_R . The renormalizability of QCD implies that all divergences can be removed in this way to all orders in perturbation theory.

5.2 Asymptotic freedom

The perturbative form (5.26) is useless for $r \rightarrow 0$ or $r \rightarrow \infty$, since then the logarithm blows up. It is useful only for r of order d , the distance scale used in the definition of the renormalized coupling constant g_R . So let us take $d = r$ from now on. Then $g_R = g_R(r)$. We can extract more information from the weak-coupling expansion by considering renormalization-group beta functions, defined by

$$\beta_R(g_R) = -r \frac{\partial}{\partial r} g_R, \quad (5.27)$$

$$\beta(g) = -a \frac{\partial}{\partial a} g. \quad (5.28)$$

It is assumed here that g_R can be considered to depend only on r and not on a – its dependence on a is compensated by the dependence on a of g . Then the r - and a -dependence on the right-hand side of (5.27) and (5.28) can be converted into a g_R - and g -dependence, respectively, using (5.25) and (5.24), giving

$$\beta_R(g_R) = -\frac{11n}{48\pi^2} g_R^3 + \dots, \quad (5.29)$$

$$\beta(g) = -\frac{11n}{48\pi^2} g^3 + \dots. \quad (5.30)$$

Actually the first *two* terms in the expansions

$$\beta(g) = -\beta_1 g^3 - \beta_2 g^5 - \beta_2 g^7 - \dots, \quad (5.31)$$

$$\beta_R(g_R) = -\beta_{R1} g_R^3 - \beta_{R2} g_R^5 - \beta_{R3} g_R^7 - \dots \quad (5.32)$$

of the two beta functions are equal. The argument for this is as follows. Let

$$g_R = F(t, g), \quad (5.33)$$

$$t = \ln\left(\frac{r^2}{a^2}\right), \quad g = g(a), \quad g_R = g_R(r), \quad (5.34)$$

Make a scale transformation $a \rightarrow \lambda a$, $r \rightarrow \lambda r$, which does not affect t , and differentiate with respect to λ , setting $\lambda = 1$ afterwards. Then $\partial/\partial\lambda = a\partial/\partial a = r\partial/\partial r$, and

$$-\beta_{\text{R}}(g_{\text{R}}) = \frac{\partial g_{\text{R}}}{\partial \lambda} = \frac{\partial F}{\partial g} \left(\frac{\partial g}{\partial \lambda} \right) = -\frac{\partial F}{\partial g} \beta(g). \quad (5.35)$$

Inserting the expansions for $\beta(g)$ and

$$g_{\text{R}} = g + F_1(t)g^3 + F_2(t)g^5 + \dots, \quad (5.36)$$

$$g = g_{\text{R}} - F_1(t)g_{\text{R}}^3 + \dots, \quad (5.37)$$

gives

$$\begin{aligned} -\beta_{\text{R}}(g_{\text{R}}) &= [1 + 3F_1g^2 + O(g^4)][\beta_1g^3 + \beta_2g^5 + O(g^7)] \\ &= [1 + 3F_1g_{\text{R}}^2 + O(g_{\text{R}}^4)][\beta_1g_{\text{R}}^3 - 3\beta_1F_1g_{\text{R}}^5 + \beta_2g_{\text{R}}^5 + O(g_{\text{R}}^7)] \\ &= \beta_1g_{\text{R}}^3 + \beta_2g_{\text{R}}^5 + O(g_{\text{R}}^7). \end{aligned} \quad (5.38)$$

Any coupling constant related to g by a series of the type (5.36) has the same beta function, so we may take the coefficient β_2 from calculations in the continuum using dimensional regularization,[†]

$$\beta_2 = \frac{102}{121}\beta_1^2, \quad \beta_1 = \frac{11n}{48\pi^2}. \quad (5.39)$$

The remarkable fact in these formulas is that the beta functions are *negative* in a neighborhood of the origin, implying that the couplings become smaller as the length scale decreases. This property is called asymptotic freedom. As we shall see, it implies that $g \rightarrow 0$ in the continuum limit. We come back to this in a later section. It suggests furthermore that perturbation theory in the renormalized coupling g_{R} becomes reliable at short distances, provided that a ‘running g_{R} ’ can be used at the appropriate length or momentum scale. In the case of the potential $V(r)$ there is only one relevant length scale, r , and we can use the r -dependence of $g_{\text{R}}(r)$ to our advantage, as will now be shown.

The precise dependence of $g_{\text{R}}(r)$ for small r follows by integrating the differential equation (5.27),

$$\begin{aligned} \frac{\partial g_{\text{R}}}{\partial \ln r} &= -\beta_{\text{R}}(g_{\text{R}}), \\ -\ln r &= \int^{g_{\text{R}}} \frac{dx}{\beta_{\text{R}}(x)} \end{aligned}$$

[†] Other authors write $\beta_{0,1}$ for our $\beta_{1,2}$.

$$\begin{aligned}
&= \int^{g_R} dx \left[\frac{-1}{\beta_1 x^3} + \frac{\beta_2}{\beta_1^2 x} + O(x) \right] \\
&= \frac{1}{2\beta_1 g_R^2} + \frac{\beta_2}{\beta_1^2} \ln g_R + \text{constant} + O(g_R^2). \quad (5.40)
\end{aligned}$$

The integration constant can be partially combined with $\ln r$ to form a dimensionless quantity $\ln(r\Lambda_V)$ in a way that has become standard:

$$-\ln(r^2 \Lambda_V^2) = \frac{1}{\beta_1 g_R^2} + \frac{\beta_2}{\beta_1^2} \ln(\beta_1 g_R^2) + O(g_R^2). \quad (5.41)$$

Note the ‘ $\ln \beta_1$ convention’. Note also that Λ_V can be defined precisely only if the β_2 term is taken into account – the $O(g_R^2)$ term no longer involves a constant term. This formula can be inverted so as to give g_R as a function of r ,

$$\beta_1 g_R^2 = \frac{1}{s} - \frac{\beta_2}{\beta_1^2} \frac{1}{s^2} \ln s + O(s^{-3} \ln s), \quad (5.42)$$

$$s = -\ln(r^2 \Lambda_V^2). \quad (5.43)$$

Inserting this into the force formula (5.23) for $d = r$ gives

$$F(r) = \frac{C_2}{4\pi r^2} \frac{\beta_1^{-1}}{s + (\beta_2/\beta_1^2)s^{-1} \ln s + O(s^{-2} \ln s)}. \quad (5.44)$$

So the short-distance behavior of the potential can be reliably computed (‘renormalization-group improved’) in QCD by means of the weak-coupling expansion. However, this expansion tells us nothing about the long-distance behavior, because $g_R(r)$ *increases* as r increases, making the first few terms of the weak-coupling expansion irrelevant in this regime.

A second important implication of asymptotic freedom is the application of the renormalization-group equation to the bare coupling g . Integration of (5.28) leads to the analog of (5.41) for the bare coupling,

$$-\ln(a^2 \Lambda_L^2) = \frac{1}{\beta_1 g^2} + \frac{\beta_2}{\beta_1^2} \ln(\beta_1 g^2) + O(g^2), \quad (5.45)$$

where we introduced the ‘lattice lambda scale’ Λ_L . The analog of (5.42),

$$\beta_1 g^2 \approx 1/|\ln(a^2 \Lambda_L^2)|, \quad (5.46)$$

shows that the bare coupling vanishes in the continuum limit $a \rightarrow 0$. This means that the critical point of the theory (the one that is physically relevant, in case there is more than one) is known: it is $g = 0$.

The inverse of (5.45) can be written as

$$\Lambda_L^2 = \frac{1}{a^2} (\beta_1 g^2)^{-\beta_2/\beta_1} e^{-1/\beta_1 g^2} [1 + O(g^2)]. \tag{5.47}$$

This equation is sometimes accompanied by the phrase ‘dimensional transmutation’: the pure gauge theory has no dimensional parameters (such as mass terms) in its classical action and we may think of transforming the bare coupling g into the dimensional lambda scale via the arbitrary regularization scale $1/a$. As we shall see later, all physical quantities with a dimension are proportional to the appropriate power of Λ_L (as in (1.4)).

The Λ_V and Λ_L are examples of the QCD lambda scales which set the physical scale of the theory. They are all proportional and their ratios can be calculated in one-loop perturbation theory. Let us see how this is done for the ratio Λ_V/Λ_L . The one-loop relation (5.25) can be rewritten as

$$\frac{1}{\beta_1 g^2} = \frac{1}{\beta_1 g_R^2} + \left[\ln \left(\frac{d^2}{a^2} \right) + c \right] + O(g_R^2). \tag{5.48}$$

Inserting this relation into (5.47) and letting a and d go to zero with d/a fixed, such that g and g_R go to zero, gives

$$\Lambda_L^2 = \frac{e^{-c}}{d^2} (\beta_1 g_R^2)^{-\beta_2/\beta_1} e^{-1/\beta_1 g_R^2} [1 + O(g_R^2)] \tag{5.49}$$

$$= \Lambda_V^2 e^{-c}. \tag{5.50}$$

Hence the ratio is determined by the constant c , which depends on the details of the regularization.

A comparison of lambda scales on the lattice and in the continuum was done some time ago [45, 46, 47]. The relation with the popular MS-bar scheme (modified minimal subtraction scheme) in dimensional renormalization is

$$\frac{\Lambda_{\overline{\text{MS}}}}{\Lambda_L} = \exp[(1/16n - 0.0849780 n)/\beta_1] \tag{5.51}$$

$$= 19.82, \quad SU(2) \tag{5.52}$$

$$= 28.81, \quad SU(3). \tag{5.53}$$

A calculation [48] of the constant c in the MS-bar scheme then gave the relation to the potential scheme Λ_V , ($\gamma = 0.57 \dots$ is Euler's constant)

$$\frac{\Lambda_V}{\Lambda_L} = \exp[\gamma - 1 - (1/16n - 0.095884 n)/\beta_1] \quad (5.54)$$

$$= 20.78, \text{ for } SU(2) \quad (5.55)$$

$$= 30.19 \text{ for } SU(3). \quad (5.56)$$

5.3 Strong-coupling expansion

The strong-coupling expansion is an expansion in powers of $1/g^2$. It has the advantage over the weak-coupling expansion that it has a non-zero radius of convergence. A lot of effort has been put into using it as a method of computation, similarly to the high-temperature or hopping expansion for scalar field theories, see e.g. [6, 44]. One has to be able to match on to coupling values where the theory exhibits continuum behavior. This turns out to be difficult for gauge theories. However, a very important aspect of the strong-coupling expansion is that it gives insight into the qualitative behavior of the theory, such as confinement and the particle spectrum. There are sophisticated methods for organizing the strong-coupling expansion, but here we give only a minimal outline of the basic ideas.

We start again with the compact $U(1)$ theory. Let p be the plaquette (x, μ, ν) , $\mu < \nu$. We write the compact $U(1)$ action in the form

$$S = \sum_p L(U_p) + \text{constant}, \quad (5.57)$$

$$L(U_p) = \frac{1}{2g^2}(U_p + U_p^*), \quad (5.58)$$

$$U_p = U_{\mu\nu}(x) = U_{\nu\mu}(x)^*. \quad (5.59)$$

In the path integral we expand $\exp S$ in powers of $1/g^2$. First consider

$$\exp \left[\frac{1}{2g^2}(U_p + U_p^*) \right] = \sum_{m,n=0}^{\infty} \frac{1}{m!n!} \left(\frac{1}{2g^2} \right)^{m+n} U_p^m U_p^{*n}. \quad (5.60)$$

Since $U_p^* = U_p^{-1}$ we put $m = n + k$ and sum over n and k , $k = 0, \pm 1, \pm 2, \dots$, which gives

$$\sum_{n=0}^{\infty} \left(\frac{1}{n!}\right)^2 \left(\frac{1}{2g^2}\right)^{2n} + (U_p + U_p^{-1}) \sum_{n=0}^{\infty} \frac{1}{(n+1)!n!} \left(\frac{1}{2g^2}\right)^{2n+1} + \dots + (U_p^k + U_p^{-k}) \sum_{n=0}^{\infty} \frac{1}{(n+k)!n!} \left(\frac{1}{2g^2}\right)^{2n+k} + \dots \tag{5.61}$$

Recognizing the modified Bessel function I_k ,

$$I_k(x) = I_{-k}(x) = \sum_{n=0}^{\infty} \frac{1}{(n+k)!n!} \left(\frac{x}{2}\right)^{2n+k}, \tag{5.62}$$

we find

$$e^{L(U_p)} = \sum_{k=-\infty}^{\infty} I_k\left(\frac{1}{g^2}\right) U_p^k. \tag{5.63}$$

This is actually an expansion of $\exp L(U_p)$ in irreducible representations of the group $U(1)$, labeled by the integer k . It is useful to extract an overall factor,

$$e^{L(U_p)} = f \sum_k a_k U_p^k, \tag{5.64}$$

$$a_k(1/g^2) = \frac{I_k(1/g^2)}{I_0(1/g^2)}, \tag{5.65}$$

$$f(1/g^2) = I_0(1/g^2). \tag{5.66}$$

The coefficients a_k are of order $(1/g^2)^k$.

Consider now the expansion of the partition function $Z = \int DU \exp S$. Using (5.57) and (5.64) we get a sum of products of U_p^k 's,

$$Z = \int DU \sum (\text{coefficient}) \prod U_p^k. \tag{5.67}$$

Each U_p^k is a product $U_1^k U_2^k U_3^{-k} U_4^{-k}$ of the four link variables U_1, \dots, U_4 of the plaquette p , raised to the power k . A given link variable belongs to $2d$ plaquettes (in d dimensions). For each link there is an integration $\int dU$ over the group manifold, which for the group $U(1)$ is simply given by

$$\int dU U^r = \int_0^{2\pi} \frac{d\theta}{2\pi} e^{ir\theta} = \delta_{r,0}, \tag{5.68}$$

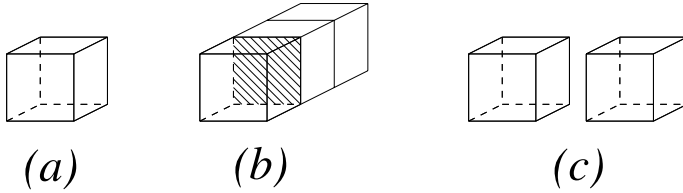


Fig. 5.7. Simple diagrams contributing to the partition function. The hatched area in (b) belongs to the closed surface. Diagram (c) is disconnected.

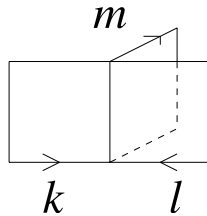


Fig. 5.8. Conservation of flux in three dimensions: $k + l + m = 0$.

where r is an integer. Hence the group integration projects out the trivial ($r = 0$) representation. Now r is the sum of the k 's belonging to the plaquettes impinging on the link under consideration. It follows that, after integration, the non-vanishing terms in (5.67) can be represented by diagrams consisting of plaquettes forming closed surfaces, as in figure 5.7. We can interpret this as follows. Each plaquette carries an amount of electric or magnetic flux (depending on its being timelike or spacelike; recall that it corresponds to a miniature line current), labeled by k . The integration over the link variables enforces conservation of flux, as illustrated in figure 5.8. If the surface is not closed, then $\int dU^r = 0$ along each link of its boundary.

Diagram (a) in figure 5.7 represents the leading contribution to Z ,

$$Z = f^{Vd(d-1)/2} \left[1 + \frac{1}{3!} Vd(d-1)(d-2) \sum_{k \neq 0} (a_k)^6 + \dots \right], \quad (5.69)$$

where V is the number of lattice sites, $Vd(d-1)/2$ is the number of plaquettes, $Vd(d-1)(d-2)/3!$ is the number of ways the cube can be embedded in the d -dimensional hypercubic lattice ($d \geq 3$) and 6 is the number of faces of the cube.

The expansion can be arranged as an expansion for $\ln Z$ containing only connected diagrams, called polymers.

For a general gauge theory the derivation of the strong-coupling expansion is similar. One writes

$$L(U_p) = \frac{\beta}{\chi_f(1)} \operatorname{Re} \chi_f(U_p), \tag{5.70}$$

where $\chi_f(U_p)$ is the character of U_p in the fundamental representation. Recall (we encountered this before in section 4.7) that these characters are orthonormal,

$$\int dU \chi_r(U) \chi_s(U)^* = \delta_{rs}, \tag{5.71}$$

and complete for class functions $F(U)$ (which satisfy $F(U) = F(VUV^{-1})$). Next $\exp L$ is written as a character expansion,

$$e^{L(U_p)} = f + f \sum_{r \neq 0} d_r a_r \chi_r(U_p), \tag{5.72}$$

where $r = 0$ denotes the trivial representation $U_p \rightarrow 1$ and $d_r = \chi_r(1)$ is the dimension of the representation r . The expansion coefficients are given by

$$f = \int dU e^{L(U)}, \tag{5.73}$$

$$d_r a_r = \frac{\int dU e^{L(U)} \chi_r^*}{\int dU e^{L(U)}}. \tag{5.74}$$

For the group $U(1)$, $r = 0, \pm 1, \pm 2, \dots$, $\beta = 1/g^2$, $\chi_r(U) = \exp(ir\theta)$ and we recover (5.65) from the integral representation of the Bessel functions

$$I_r(x) = \frac{1}{\pi} \int_0^\pi d\theta \cos(k\theta) e^{x \cos \theta}. \tag{5.75}$$

For the group $SU(n)$, $\chi_f(1) = n$ and

$$\beta = 2n/g^2. \tag{5.76}$$

The leading β -dependence of $a_f(\beta)$ is easily found,

$$\begin{aligned} f(\beta) &= \int dU e^{(\beta/2n)(\chi_f + \chi_f^*)} \\ &= 1 + O(\beta^2), \\ na_f(\beta) &= f(\beta)^{-1} \int dU e^{(\beta/2n)(\chi_f + \chi_f^*)} \chi_f^* \end{aligned} \tag{5.77}$$

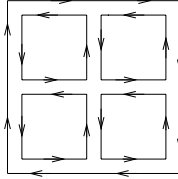


Fig. 5.9. A small Wilson loop with compensating plaquettes.

$$= \frac{\beta}{2n} + O(\beta^2), \quad n > 2 \tag{5.78}$$

$$= \frac{\beta}{n} + O(\beta^2), \quad n = 2. \tag{5.79}$$

For $SU(2)$ the characters are real. In terms of g^2 ,

$$a_f = \frac{1}{g^2} + \dots, \quad n = 2, \tag{5.80}$$

$$= \frac{1}{ng^2} + \dots, \quad n = 3, 4, \dots \tag{5.81}$$

Up to group-theoretical complications (which can be formidable) the strong-coupling expansion for general gauge groups follows that of the $U(1)$ case. The graphs are the same, but the coefficients differ.

5.4 Potential at strong coupling

We now turn to the expectation value of the rectangular Wilson loop $\langle U(C) \rangle$, from which the potential can be calculated. The links on the curve C contain explicit factors of U that have to be compensated by plaquettes from the expansion of $\exp S$, otherwise the integration over U gives zero. Figure 5.9 shows a simple example. The contribution of this diagram is (the Wilson loop is taken in the fundamental representation of $U(1)$)

$$[a_1(1/g^2)]^4, \tag{5.82}$$

which is the leading contribution for this curve C . Recall that a_1 is given by

$$a_1(1/g^2) = \frac{I_1(1/g^2)}{I_0(1/g^2)} = \frac{1}{2g^2} - \frac{1}{2} \left(\frac{1}{2g^2} \right)^3 + \dots \tag{5.83}$$

In higher orders disconnected diagrams appear. It can be shown, however, that disconnected diagrams may be discarded: they cancel out

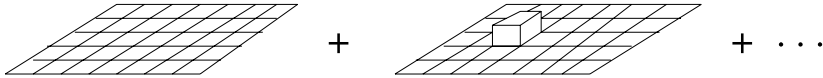


Fig. 5.10. Leading diagrams for a large Wilson loop.

between the numerator and denominator of $\langle U(C) \rangle$. The expansion can be rewritten as a sum of connected diagrams. Figure 5.10 illustrates the leading terms for a large Wilson loop,

$$W(r, t) = a_1^A + 2(d - 2)Aa_1^{A+4} + \dots, \tag{5.84}$$

where A is the area of the loop, in lattice units $A = rt$. Boundary corrections are also in the \dots . The higher orders correspond to ‘decorations’ of the minimal surface.

The potential $V(r)$ follows now from (5.1) and $A = rt$,

$$\begin{aligned} V(r) &= \frac{1}{t} \ln W(r, t) \\ &= -[\ln a_1 + 2(d - 2)a_1^4 + \dots] r. \end{aligned} \tag{5.85}$$

For $r \rightarrow \infty$, $A \rightarrow \infty$ and the boundary corrections become negligible. Hence, the potential is *linearly confining* at large distances,

$$V(r) \approx \sigma r, \quad r \rightarrow \infty, \tag{5.86}$$

$$\sigma = -\ln a_1 - 2(d - 2)a_1^4 + \dots. \tag{5.87}$$

At strong coupling the compact $U(1)$ theory is confining.

For other gauge theories the calculation of the leading contribution to a Wilson loop in the fundamental representation goes similarly. A useful formula here is

$$\int dU \chi_r(UV)\chi_s(W^\dagger U^\dagger) = \frac{\delta_{rs}}{d_r} \chi_r(VW^\dagger), \tag{5.88}$$

which follows from

$$\int dU \mathcal{D}_{mn}^r(U) \mathcal{D}_{m'n'}^{r'}(U)^* = \delta_{rr'} \delta_{mm'} \delta_{nn'} \frac{1}{d_r}, \tag{5.89}$$

seen earlier in (4.145). The use of this formula is illustrated in figure 5.11. Successive integration in the simple Wilson-loop example in figure 5.9 is illustrated in figure 5.12. Each arrow in figure 5.12 denotes the result of ‘integrating out a link’. The equality signs symbolize $UU^\dagger = 1$. Note that the factors d_r in (5.88) cancel out with those in (5.72). Hence

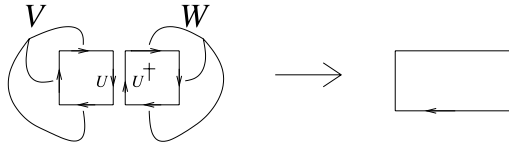


Fig. 5.11. Integration of a link variable.

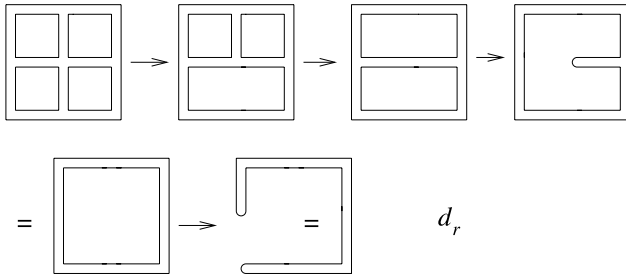


Fig. 5.12. Integrating the leading contribution to a 2×2 Wilson loop.

the numerical value of the diagram is $d_r a_r(\beta)^4$, for a Wilson loop in representation r .

Another way to see this is as follows: in figure 5.9 there are $n_l = 12$ links, $n_p = 4$ plaquettes and $n_s = 9$ sites. Integrating over each link gives a factor $d_r^{-n_l}$ by (5.89) and contracting the Kronecker deltas at each site gives a factor $d_r^{n_s}$. Each plaquette has a factor $d_r^{n_p}$ by (5.72). For a simple surface without handles, the Euler number is

$$-n_l + n_s + n_p = 1$$

$$\Rightarrow \text{leading contribution} = (d_r)^{-n_l+n_s} [d_r a_r(\beta)]^{n_p} = d_r a_r(\beta)^{n_p}. \quad (5.90)$$

For a Wilson loop in the fundamental representation of the $SU(n)$ theory the first few terms in the expansion for the string tension

$$\sigma = -\ln a_f(\beta) - 2(d-2)a_f(\beta)^4 + \dots \quad (5.91)$$

are similar to the $U(1)$ result (5.87). In higher orders the $a_r(\beta)$ corresponding to other irreps enter. The final result may then be re-expressed by expansion in powers of $1/ng^2$.

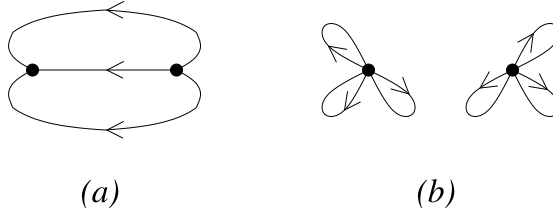


Fig. 5.13. Flux lines for sources in the fundamental (a) and the adjoint (b) representation.

5.5 Confinement versus screening

In the previous section we saw that the $U(1)$ and $SU(n)$ potentials are confining in the strong-coupling region. From the derivation we can see that this is true for external charges (Wilson loops) in the fundamental representation of any compact gauge group. However, external charges in the *adjoint* representation of $SU(n)$ are *not* confined. This is because the charges in the adjoint representation can be *screened* by the gauge field. A adjoint source is like a quark–antiquark pair, as illustrated intuitively in figure 5.13. We now show how this happens at strong coupling.

Let U denote the fundamental representation (as before) and R the adjoint representation. The latter can be constructed from U and U^\dagger ,

$$R_{kl} = 2 \operatorname{Tr}(U^\dagger t_k U t_l), \tag{5.92}$$

where the t_k are the generators in the fundamental representation. Since R is an irrep,

$$\int dU R_{kl}(U) = 0. \tag{5.93}$$

To compensate the R 's on the links of the adjoint Wilson loop

$$\operatorname{Tr} R(C) = \operatorname{Tr} \prod_{l \in C} R_l \tag{5.94}$$

by the plaquettes from the expansion of $\exp S$, we may draw a Wilson surface and find in the same way as in the previous section the seemingly leading contribution

$$d_a a_a(\beta)^A, \quad d_a = n^2 - 1, \tag{5.95}$$

with A the minimal surface spanned by C . However, there is a more economical possibility for large A , illustrated in figure 5.14. The tube of plaquettes is able to screen the adjoint loop. To evaluate this contribution we unfold the tube as in figure 5.15. The links in the interior

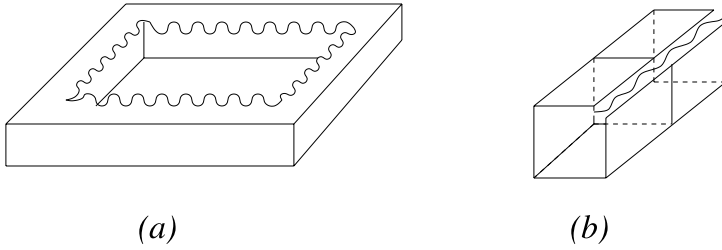


Fig. 5.14. Diagram contributing to a Wilson loop in the adjoint representation; (b) is a close up of a piece of the circumference in (a). The wavy line indicates the adjoint representation.

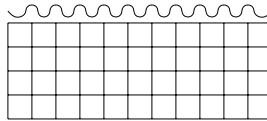


Fig. 5.15. Unfolding the tube of plaquettes. The horizontal and vertical boundaries are to be identified.

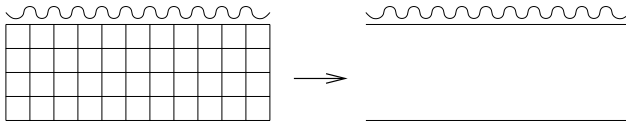


Fig. 5.16. Integrating out the interior.

can be integrated out as in figure 5.12, as illustrated in figure 5.16. The first step gives a factor $d_f a_f(\beta)^{N_p}$ with N_p the number of plaquettes ($d_f = n$). The second step gives an additional factor $1/d_f$. There remains the integration over the links of the Wilson loop, which leads to integrals of the type (for $n \geq 3$) (cf. (A.93) in appendix A.4)

$$\int dU U_b^a U_p^{q\dagger} R_{kl} = \frac{1}{d_a} 2(t_k)_p^a (t_l)_b^q, \quad n > 2, \tag{5.96}$$

as illustrated in figure 5.17. So we get a trace of the form

$$2d_a^{-1} (t_k)_p^a (t_l)_b^q 2d_a^{-1} (t_l)_q^b (t_m)_c^r \cdots (t_k)_a^p = 1, \tag{5.97}$$

since $2 \text{Tr} (t_k t_k) = n^2 - 1 = d_a$. This leads to a factor

$$a_f(\beta)^{4P}, \tag{5.98}$$

where P is the perimeter of the (large) adjoint loop in lattice units:

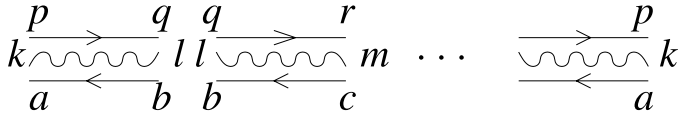


Fig. 5.17. Link variables on the adjoint loop.

$P = 2(r + t)$, and the factor 4 in the exponent reflects the fact that there are four plaquettes per unit length.

The leading contributions of the perimeter and area type in the $SU(n)$ theory are given by

$$W_a(r, t) \sim (n^2 - 1)(a_a)^{rt} + \dots + 2(d - 1)(d - 2)(a_f)^{8(r+t)} + \dots, \tag{5.99}$$

which by (5.1) leads to a potential

$$\begin{aligned} V(r) &= \sigma_{\text{eff}} r, \quad r \leq \frac{V(\infty)}{\sigma_{\text{eff}}} \\ &= V(\infty), \quad r \geq \frac{V(\infty)}{\sigma_{\text{eff}}}, \end{aligned} \tag{5.100}$$

with

$$\sigma_{\text{eff}} = -\ln a_a + \dots, \tag{5.101}$$

$$V(\infty) = -8 \ln a_f + \dots, \tag{5.102}$$

$$\begin{aligned} a_f &= (ng^2)^{-1} + \dots, \\ a_a &= \frac{n^2}{n^2 - 1} (ng^2)^{-2} + \dots. \end{aligned} \tag{5.103}$$

(This behavior of a_a follows easily from (5.74) and (5.96).)

At large distances the potential approaches a constant. The sharp crossover from linear to constant behavior (at $r \approx 4$) is an artifact of our simplistic strong-coupling calculation. Still, the calculation suggests that there is an intermediate region where the potential is approximately linear with some effective string tension σ_{eff} , although strictly speaking the string tension, defined by $\sigma = V(r)/r$, $r \rightarrow \infty$, vanishes for adjoint sources.

To decide whether static charges in an irreducible representation r can be screened by the gauge field, we consider the generalization of (5.96),

$$I = \int dU \mathcal{D}_{mn}^s(U) \mathcal{D}_{m'n'}^s(U)^* \mathcal{D}_{kl}^r(U), \tag{5.104}$$

where s denotes the irreps of the two screening plaquettes. If the integral I is zero, the source cannot be screened, and vice-versa. Let Z_k denote an element of the center of $SU(n)$, i.e. $Z_k \in SU(n)$ commutes with all group elements and it is represented in the fundamental representation as a multiple of the identity matrix,

$$(Z_k)_b^a = e^{ik2\pi/n} \delta_b^a, \quad k = 0, 1, \dots, n-1. \quad (5.105)$$

Irreps r can be constructed from a tensor product $U \otimes U \cdots U \otimes U^\dagger \cdots \otimes U^\dagger$, say p times U and q times U^\dagger , so r can be assigned an integer $\nu(r) = p - q \bmod n$, from the way it transforms under $U \rightarrow Z_1 U$:

$$\mathcal{D}_{kl}^r(Z_1 U) \rightarrow e^{i\nu(r)2\pi/n} \mathcal{D}_{kl}^r(U). \quad (5.106)$$

The integer $\nu(r)$ is called the n -ality of the representation (trality for $n = 3$). Making the change of variables $U \rightarrow Z_1 U$ in (5.104) gives

$$I = e^{i\nu(r)2\pi/n} I, \quad (5.107)$$

and we conclude that $I = 0$ if the n -ality $\nu(r) \neq 0$. Sources with non-zero n -ality are confined; sources with zero n -ality are not confined. In QCD, static quarks have non-zero trality and are confined.

5.6 Glueballs

The particles of the pure gauge theory are called glueballs. They may be interpreted as bound states of gluons. Gluons appear as a sort of photons in the weak-coupling expansion and, because of asymptotic freedom, they manifest themselves as effective particle-like excitations at high energies. However, gluons do not exist as free particles because of confinement, as we shall see.

Masses of particles can be calculated from the long-distance behavior of suitable fields. These are gauge-invariant fields constructed out of the link variables $U_{\mu x}$, such as Wilson loops, with the quantum numbers of the particles being studied. The transfer-matrix formalism shows that an arbitrary state can be created out of the vacuum by application of a suitable combination of spacelike Wilson loops. The simplest of these is the plaquette field $\text{Tr} U_{mnx}$, $m, n = 1, 2, 3$. The plaquette-plaquette expectation value (4.97) can be calculated easily at strong coupling. The relevant diagrams consist of tubes of plaquettes, as in figure 5.18. Since there are four plaquettes per unit of time, the glueball mass is given by $m = -4 \ln a_f(\beta) + \dots$. The higher-order corrections correspond to

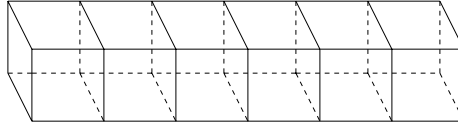


Fig. 5.18. The leading strong-coupling diagram for the plaquette–plaquette correlator. Time runs horizontally.

diagrams decorating the basic tube of figure 5.18, which will also cause the tube to perform random walks.

The plaquette can be decomposed into operators with definite quantum numbers under the symmetry group of the lattice, and such operators can in turn be embedded into representations of the continuum rotation group of spin zero, one and two. To be more precise, the quantum numbers J^{PC} (J = spin, P = parity, C = charge-conjugation parity) excited by the plaquette are 0^{++} , 1^{+-} and 2^{++} , which may be called scalar (S), axial vector (A) and tensor (T). The description of glueballs with other quantum numbers requires more complicated Wilson loops. The terms in the strong-coupling series

$$m_j = -4 \ln u + \sum_k m_j^k u^k, \quad j = S, A, T, \quad u \equiv a_f(\beta), \quad (5.108)$$

have been calculated to order u^8 for gauge groups $SU(2)$ and $SU(3)$ [91, 92]. See [10] for details.

Since the strong-coupling diagrams are independent of the (compact) gauge group (but their numerical values are not), also the $U(1)$ and e.g. $Z(n)$ gauge theories† have a particle content at strong coupling similar to that of glueballs.

5.7 Coulomb phase, confinement phase

We have seen that all gauge theories with a compact gauge group such as $U(1)$, $SU(n)$ and $Z(n)$ have the property of confinement at strong coupling, and the emerging particles are ‘glueballs’. On the other hand, we have also given arguments, for $U(1)$ and $SU(n)$, that the weak-coupling expansion on the lattice gives the usual universal results for renormalized quantities found with perturbation theory in the continuum.

In particular the compact $U(1)$ theory at weak coupling is not confining and it contains no glueballs but simply the photons of the free

† $Z(n)$ is the discrete group consisting of the center elements (5.105) of $SU(n)$.

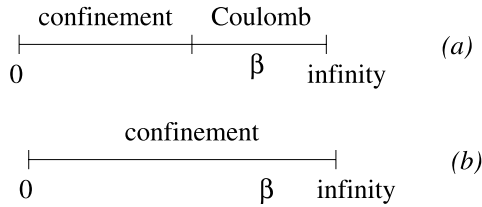


Fig. 5.19. Phase diagram of the compact $U(1)$ gauge theory (a) and the $SU(n)$ gauge theory, $n = 2, 3$ (b).

Maxwell theory. The physics of the compact $U(1)$ theory is clearly different in the weak- and strong-coupling regions. This can be understood from the fact that there is a phase transition as a function of the bare coupling constant (figure 5.19). One speaks of a Coulomb phase at weak coupling and a confining phase at strong coupling. In the Coulomb phase the static potential has the standard Coulomb form $V = -g_R^2/4\pi r + \text{constant}$, whereas in the confinement phase the potential is linearly confining at large distances, $V \approx \sigma r$. There is a phase transition at a critical coupling $\beta_c \equiv 1/g_c^2 \approx 1.01$, at which the string tension $\sigma(\beta)$ vanishes; see for example [95].

The Wilson loop serves as an order field in pure gauge theories. Consider a rectangular $r \times t$ Wilson loop C , with perimeter $P = 2(r + t)$ and area $A = rt$. When the loop size is scaled up to infinity, the dominant behavior is a decay according to a perimeter law or an area law:

$$W(C) \sim e^{-\epsilon P}, \text{ Coulomb phase,} \quad (5.109)$$

$$W(C) \sim e^{-\sigma A}, \text{ confinement phase.} \quad (5.110)$$

Here ϵ may be interpreted as the self-energy of a particle tracing out the path C in (Euclidean) space-time, and σ is the string tension experienced by a particle.

There is no phase transition in the $SU(2)$ and $SU(3)$ models with the standard plaquette action in the fundamental representation in the whole region $0 < \beta < \infty$ ($\beta = 2n/g^2$). This conclusion is based primarily on numerical evidence (see e.g. the collection of articles in [5]) and it is also supported by analytic mean-field calculations (see e.g. [6] for a review). The absence of a phase transition, combined with confinement at strong coupling, may be interpreted as evidence for confinement also in the weak-coupling region.

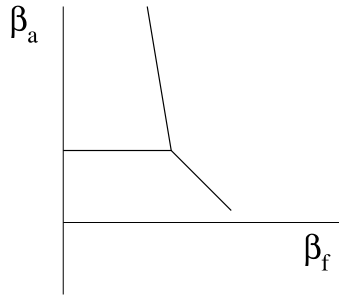


Fig. 5.20. Qualitative phase diagram of mixed-action $SU(n)$ gauge theory for $n = 2, 3$.

It should be kept in mind that the phase structure of a theory is not universal and depends on the action chosen. Only the scaling region near a critical point is supposed to have universal properties. For example, in $SU(n)$ gauge theory with an action consisting of a term in the fundamental representation and a term in the adjoint representation,

$$S = \sum_p [\beta_f d_f^{-1} \text{Re Tr } U_p + \beta_a d_a^{-1} \text{Re Tr } D^a(U_p)], \quad (5.111)$$

the phase diagram in the β_f - β_a coupling plane looks schematically like figure 5.20. This figure shows two connected phase regions; the one relevant for QCD is the region connected to the weak-coupling region $\beta_f/2n + \beta_a n/(n^2 - 1) = 1/g^2 \rightarrow \infty$ (recall (4.85)). For $n > 3$ the phase boundary going downward in the south-east direction crosses the β_f axis. This implies that, for $n > 3$, the model with only the standard plaquette action in the fundamental representation shows a phase transition. It is, however, not a deconfining transition because we can go around it continuously through negative values of the adjoint coupling β_a .

The phase structure of lattice gauge theories is rich subject and for more information we refer the reader to [5] and [6], and [10].

5.8 Mechanisms of confinement

As we have seen in section 5.1, the calculation of the static potential from a Wilson loop to lowest order of perturbation in g^2 gives a Coulomb potential. In the compact $U(1)$ theory, higher orders did not change this result qualitatively, whereas in $SU(n)$ gauge theory, there are logarithmic corrections, that can be interpreted in terms of asymptotic freedom.

However, there is no sign of confinement in weak-coupling perturbation theory. This can be understood from the fact that we expect the string tension to depend on the bare coupling g^2 as

$$\sqrt{\sigma} = C_\sigma \Lambda_L = C_\sigma \frac{1}{a} (\beta_1 g^2)^{-\beta_2/2\beta_1^2} e^{-1/\beta_1 g^2} [1 + O(g^2)], \quad (5.112)$$

which has no weak-coupling expansion (all derivatives $\partial/\partial g^2$ vanish at $g = 0$). The physical region is at weak coupling, where the lattice spacing is small, so how can we understand confinement in this region?

Non-perturbative field configurations have long been suspected to do the job. Such configurations are fundamentally different from mere fluctuations on a zero or pure-gauge background. We mention here in particular *magnetic-monopole* configurations envisioned by Nambu [49], 't Hooft [50], and Polyakov [41], and *Z(n) vortex* configurations put forward by 't Hooft [51] and Mack [52].

It can be shown that the confinement of the compact $U(1)$ theory is due to the fact that it is really a theory of photons interacting with magnetic monopoles (see e.g. the first reference in [53] for a review). These monopoles *condense* in the confinement phase in which the model behaves like a *dual superconductor*. In a standard type-II superconductor, electrically charged Cooper pairs are condensed in the ground state, which phenomenon causes magnetic-field lines to be concentrated into line-like structures, called Abrikosov flux tubes. Magnetic monopoles, if they were to exist, would be confined in such a superconductor, because the energy in the magnetic flux tube between a monopole and an antimonopole would increase linearly with the distance between them.

In a dual superconductor electric and magnetic properties are interchanged. The compact $U(1)$ model is a dual superconductor in the strong-coupling phase, in which the magnetically charged monopoles condense and the electric-field lines are concentrated in tubes, such that the energy between a pair of positively and negatively charged particles increases linearly with distance. In this way the model is an illustration of the dual-superconductor hypothesis as the explanation of confinement in QCD.

At weak coupling the monopoles decouple in the compact $U(1)$ model, because they are point particles that acquire a Coulomb self-mass of order of the inverse lattice spacing a^{-1} . However, in $SU(2)$ gauge theory, according to [53], there are 'fat' monopoles that have physical sizes and masses, and do not decouple at weak bare gauge coupling g^2 . They remain condensed as $g^2 \rightarrow 0$ and continue to produce a non-zero string

tension for all values of g^2 . A similar mechanism is supposed to take place in $SU(n)$ gauge theory for $n > 2$.

The mechanism for confinement in $SU(n)$ gauge theory proposed by Mack is condensation of fat $Z(n)$ vortices. The latter cause an area-type decay of large Wilson loops in much the same way as in the $Z(n)$ gauge theory at strong coupling.

There seems to be more than one explanation of confinement, depending on the gauge one chooses to work in. This may seem disturbing, but, e.g. also in scattering processes, different reference frames (such as ‘center of mass’ or ‘laboratory’) lead to different physical pictures. Numerical simulations offer a great help in studying these fundamental questions. Lattice XX reviews are in [54], see also [55, 56, 57, 58, 59].

5.9 Scaling and asymptotic scaling, numerical results

We say that relations between physical quantities scale if they become independent of the correlation length ξ as it increases toward infinity. In practice this means once ξ is sufficiently large. In pure $SU(n)$ gauge theory the correlation length is given by the mass in lattice units of the lightest glueball, $\xi = 1/am$. For instance, glueball-mass ratios m_i/m_j are said to scale when they become approximately independent of ξ . Typically one expects corrections of order a^2 ,

$$m_i/m_j = r_{ij} + r'_{ij}a^2m^2 + O(a^4). \quad (5.113)$$

For the usual plaquette action am is only a function of the bare gauge coupling g^2 . We can write $m = C_m\Lambda_L$, with Λ_L the lambda scale introduced in (5.45) and C_m a numerical constant characterizing the glueball. The correlation length is then related to the gauge coupling by

$$\xi_m^{-2} = a^2m^2 = C_m^2 a^2\Lambda_L^2 = C_m^2 (\beta_1 g^2)^{-\beta_2/\beta_1^2} e^{-1/\beta_1 g^2} [1 + O(g^2)], \quad (5.114)$$

for sufficiently small g^2 . Neglecting the $O(g^2)$, this behavior as a function of g^2 is called asymptotic scaling.

It turns out that asymptotic scaling is a much stronger property than scaling, in the sense that scaling may set in when the correlation length is only a few lattice spacings, whereas asymptotic scaling is not very well satisfied yet. In the usual range of couplings, which are of order $\beta = 2n/g^2 = 6$ for $SU(3)$ gauge theory with the plaquette action in the fundamental representation, once $\beta \geq 5.7$ or so, the correlation length appears to be sufficiently large and the $O(a^4)$ corrections small enough

for scaling corrections to be under control. However, asymptotic scaling does not hold very well yet in this region. Apparently the $O(g^2)$ corrections in (5.114) cannot be neglected. This has led to a search for ‘better’ expansion parameters, i.e. ‘improved’ definitions of a bare coupling that may give better convergence, see e.g. [60]. Note that $\exp(-1/\beta_1 g^2)$ is a rapidly varying function of g^2 because $\beta_1 = 11n/48\pi^2 \approx 0.070$ ($n = 3$) is so small. Typically $\Delta\beta \approx 0.48$ corresponds to a reduction of a^2 by a factor of four near $\beta = 6$.

The potential $V(r)$ is a good quantity to test for scaling because it is relatively easy to compute and there are many values $V(r)$. As a measure of the correlation length we may take

$$\xi_\sigma(\beta) = 1/a\sqrt{\sigma}, \tag{5.115}$$

where $a^2\sigma$ is the string tension in lattice units, which goes to zero as β approaches infinity. Assuming $\sqrt{\sigma} = 400$ MeV, for example (cf. section 1.1), the value of $a\sqrt{\sigma}$ give us the lattice distance a in units $(\text{MeV})^{-1}$. This can be used to express the potential in physical units as follows. The potential in lattice units can be written as

$$aV = v\left(\frac{r}{a}, \beta\right), \tag{5.116}$$

where v is a function of the dimensionless variables r/a and β . Recall that V contains the unphysical self-energy of the sources, which is distance independent. Expressing the potential in physical units, as set by the string tension, gives

$$\frac{V}{\sqrt{\sigma}} = \xi_\sigma(\beta) v\left(\frac{r\sqrt{\sigma}}{\xi_\sigma(\beta)}, \beta\right) \equiv \tilde{V}(r\sqrt{\sigma}, \beta) + v_0(\beta). \tag{5.117}$$

These relations ‘scale’ when \tilde{V} becomes independent of β . Here $v_0(\beta)$ is the self-energy, which can be fixed by a suitable choice of the zero point of energy, e.g. $\tilde{V}(1) = 0$. In practice, after computing σ from the long-distance behavior $V \approx \sigma r + \text{constant} + O(r^{-1})$, the data points at various $\beta \geq 6$ can be made to form a single scaling curve by plotting $V/\sqrt{\sigma}$ versus $r\sqrt{\sigma}$ with a suitable vertical shift corresponding to $v_0(\beta)$.

However, the accuracy of such scaling tests is limited by the fact that σ is an asymptotic quantity defined in terms of the behavior of the potential at infinity. This problem may be circumvented by concentrating on the force $F = \partial V/\partial r$, in terms of which we can define a reference distance r_0 by

$$r_0^2 F(r_0) = 1.65. \tag{5.118}$$

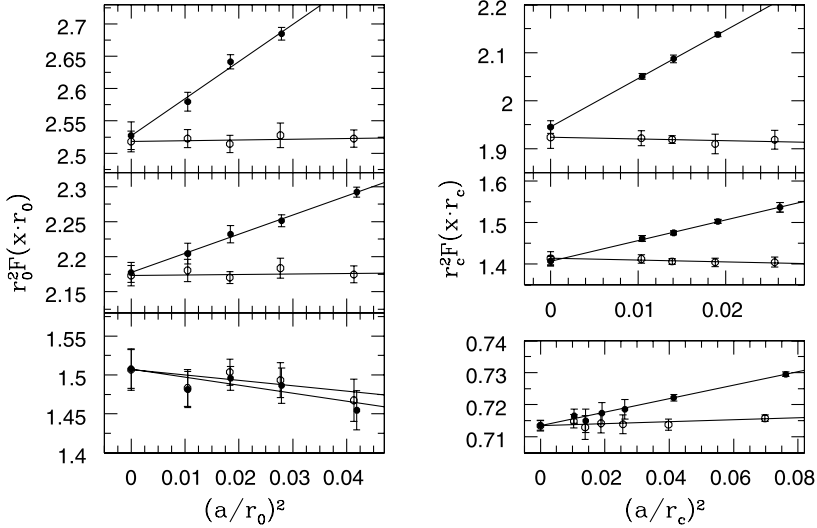


Fig. 5.21. Scaling of the $SU(3)$ force and the continuum limit at $x = r/r_0 = 0.4, 0.5,$ and 0.9 (left), and $x = r/r_c = 0.5, 0.6,$ and 1.5 (right) from top to bottom. The stronger/weaker dependence on a corresponds to r_1 defined in (5.119)/(5.120). From [62].

The choice 1.65 turns out to give $r_0 \approx 1/\sqrt{\sigma}$, which is in the intermediate-distance regime within which the potential and force can be computed accurately [61]. The force may be computed as

$$F(r_1) = [V(r + a) - V(r)]/a, \quad r_1 = r - a/2, \tag{5.119}$$

and scaling tests can then be performed as above with $\sqrt{\sigma} \rightarrow 1/r_0$. There is another choice for r_1 that gives an improved definition of the force, leading to much smaller scaling violations in the small- and intermediate-distance region [61], namely

$$(4\pi r_1)^{-2} = [v(r_1, 0, 0) - v(r_1 - a, 0, 0)]/a, \tag{5.120}$$

where $v(x, y, z)$ is the lattice Coulomb potential (5.11). The scaling test for the force avoids ambiguities from the Coulomb self-energy in the potential. Writing $r = xr_0$, or $r = xr_c$, where r_c is defined as in (5.118) with $1.65 \rightarrow 0.65$, a scaling analysis is carried out in [62] in the form $r_0^2 F(xr_0) = f_0(x) + f'_0(a/r_0)^2 + O(a^4)$, or with $r_0 \rightarrow r_c$, as shown in figure 5.21. The values of $(a/r_{0,c})^2$ correspond to β in the interval [5.7, 6.92].

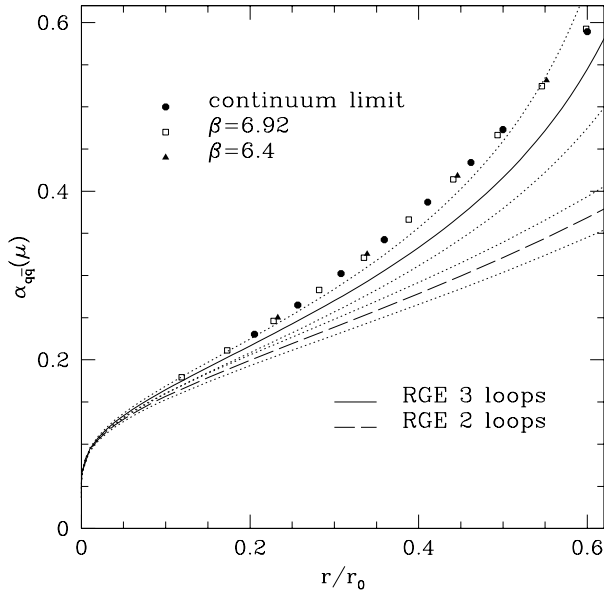


Fig. 5.22. The running coupling $\alpha_{q\bar{q}}(\mu) = g_R^2(\mu)/4\pi$, $\mu = 1/r$ plotted versus r/r_0 and compared with the dependence on r as predicted by the weak-coupling expansion for the renormalization-group beta function (the curves labeled RGE; dotted lines correspond to 1σ uncertainties of $\Lambda_{\overline{\text{MS}}}(r_0)$). From [64].

In the small-distance regime the running of the coupling (5.23), i.e. $g_R^2(\mu) = 4\pi r^2 F(r)/C_2$, $\mu = 1/r$, can be compared with the prediction of the perturbative beta function, which is known to three-loop order. One could use the perturbative expansion (5.41) in which Λ_V , or equivalently $\Lambda_{\overline{\text{MS}}}$, appears as an integration constant. This scale in units of r_0 , i.e. $r_0\Lambda_{\overline{\text{MS}}}$, has been determined independently in an elaborate non-perturbative renormalization-group computation [63]. Instead of using the perturbative expansion it is more accurate to integrate the two- or three-loop renormalization-group equation numerically. The result is shown in figure 5.22, where we see that perturbation theory works surprisingly well, when it is implemented in this way, up to quite large α 's. In physical units $r_0 \approx 1/\sqrt{\sigma} \approx 0.5$ fm.

Note that knowledge of a non-perturbative Λ scale allows the *prediction* of α_s . Such a program has been pursued in full QCD in various ways [66] and the resulting α_s agrees well with the experimentally measured values, see also the review in [2].

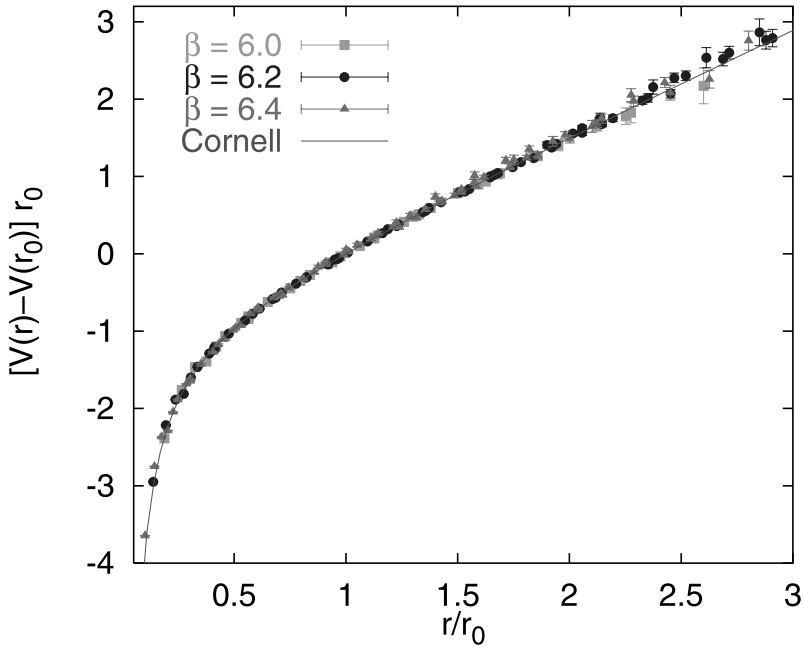


Fig. 5.23. The potential from two values of β . The curve labeled ‘Cornell’ is a fit of the form $-\frac{4}{3}\alpha/r + \text{constant} + \sigma r$ with constant α . From [65].

An overview of numerically computed potential is given in figure 5.23.

Glueball masses have by now also been computed with good accuracy in the $SU(n)$ models, using variational methods for determining the eigenvalues of the transfer matrix. It is particularly interesting to do this for varying n , since the theory simplifies in the large- n limit in the sense that only planar diagrams contribute [67]. The same is true in the strong-coupling expansion [68]. Figure 5.24 shows recent results for various n . We see that ratios with $\sqrt{\sigma}$ do indeed behave smoothly as a function of $1/n^2$ all the way down to $n = 2$.

Last, but not least, *analytic* computations in *finite volume* are theoretically very interesting and a comparison with numerical data is very rewarding. For a review, see [18].

5.10 Problems

(i) *Gauge fixing and the weak-coupling expansion*

Consider a partition function for a $U(1)$ or $SU(n)$ lattice gauge-

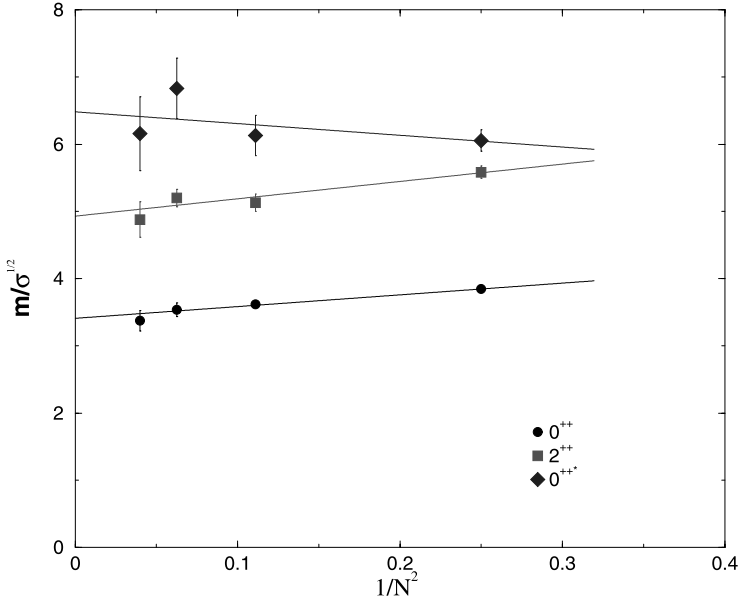


Fig. 5.24. Ratios of glueball masses with $\sqrt{\sigma}$, extrapolated to $a \rightarrow 0$ and infinite volume, as a function of $1/n^2$, for $n = 2, 3, 4, 5$. From [69].

field theory with gauge-invariant action $S(U)$,

$$Z = \int DU \exp[S(U)]. \tag{5.121}$$

The action may be the standard plaquette action

$$S(U) = -\frac{1}{2\rho g^2} \sum_{x\mu\nu} \text{Tr} (1 - U_{\mu\nu x}), \tag{5.122}$$

it may also contain the effect of dynamical fermions in the form $\ln \det A(U)$, with A the ‘fermion matrix’, cf. section 7.1. Let $O(U)$ be a gauge-invariant observable, $O(U) = O(U^\Omega)$,

$$U_{\mu x}^\Omega = \Omega_x U_{\mu x} \Omega_{x+\hat{\mu}}^\dagger, \tag{5.123}$$

and

$$\langle O \rangle = \frac{\int DU \exp[S(U)] O(U)}{Z}. \tag{5.124}$$

be the average of O .

We want to evaluate the path integrals in the weak-coupling expansion and expect to use gauge fixing, as in the

continuum. We can try to restrict the implicit integration over all gauge transformations in $\langle O \rangle$, loosely called gauge fixing, by adding an action $S_{\text{gf}}(U)$ to $S(U)$ that is not invariant under gauge transformations. For example,

$$S_{\text{gf}}(U) = -\frac{1}{\xi} \sum_x \frac{1}{2g^2\rho} \text{Tr}(\partial'_\mu \text{Im} U_{\mu x})^2, \quad \text{Im} U \equiv \frac{U - U^\dagger}{2i}, \tag{5.125}$$

with $\partial'_\mu = -\partial_\mu^\dagger$ the backward derivative, $\partial'_\mu f_x = f_x - f_{x+\hat{\mu}}$. Let $\Delta(U)$ be defined by

$$\Delta(U)^{-1} = \int D\Omega \exp[S_{\text{gf}}(U^\Omega)], \tag{5.126}$$

where $\int D\Omega$ is the integration over all gauge transformations. It is assumed that $\Delta(U)^{-1} \neq 0$.

(a) Show that the Faddeev–Popov measure factor $\Delta(U)$ is gauge invariant.

We insert $1 = \Delta(U) \int D\Omega \exp[S_{\text{gf}}(U^\Omega)]$ into the integrands in the above path-integral expression for $\langle O \rangle$ and make a transformation of variables $U \rightarrow U^{\Omega^\dagger}$. Using the gauge invariance of $S(U)$, $O(U)$, and $\Delta(U)$ we get

$$\begin{aligned} \langle O \rangle &= \frac{\int D\Omega \int DU \Delta(U) \exp[S(U) + S_{\text{gf}}(U)] O(U)}{\int D\Omega \int DU \Delta(U) \exp[S(U) + S_{\text{gf}}(U)]} \\ &= \frac{\int DU \Delta(U) \exp[S(U) + S_{\text{gf}}(U)] O(U)}{\int DU \Delta(U) \exp[S(U) + S_{\text{gf}}(U)]}. \end{aligned} \tag{5.127}$$

In the weak-coupling expansion we expand about the saddle points with maximum action. We assume this maximum to be given by $U_{\mu x} = 1$. There will in general be more maxima. For example, without dynamical fermions, $U_{\mu x} = U$ (i.e. independent of x and μ) and $U_{\mu x} = Z_\mu$, with Z_μ an element of the center of the gauge group, give the same value of the plaquette action as does $U_{\mu x} = 1$. Intuitively we expect constant modes to be important for finite-size effects, but not important in the limit that the space–time volume goes to infinity. Restricting ourselves here to the latter case, we shall not integrate over constant modes and expand about $U_{\mu x} = 1$, writing

$$U_{\mu x} = \exp(-igA_{\mu x}^k t_k). \tag{5.128}$$

The evaluation of the integral (5.126) defining $\Delta(U)$ is also done perturbatively. Because of the factor $1/g^2$ in the gauge-fixing

action, we only need to know $\Delta(U)$ for small $\partial'_\mu \text{Im Tr } U_{\mu x}$. The integral (5.126) has a saddle point at $\Omega_x = 1$, but there are in general many more saddle points Ω_x , called Gribov copies, with $S_{\text{gf}}(U^\Omega) = S_{\text{gf}}(U)$. The study of Gribov copies is complicated. One can give arguments that the correct weak-coupling expansion is obtained by restriction to the standard choice $\Omega_x = 1$, and this is what we shall do in the following. This means that, for the perturbative evaluation of $\Delta(U)$, we can write

$$\Omega_x = \exp(i g \omega_x^k t_k) \tag{5.129}$$

and expand in $g\omega_x$. In perturbation theory we may just as well simplify the gauge-fixing action and use

$$S_{\text{gf}} = -\frac{1}{2\xi^2} \sum_x \partial'_\mu A_{\mu x}^k \partial'_\nu A_{\nu x}^k. \tag{5.130}$$

(In the neighborhood of the identity, $A_{\mu x}^k$ and ω_x^k are well defined in terms of $U_{\mu x}$ and Ω_x .)

We extend the initially compact integration region over $A_{\mu x}^k$ and ω_x^k to the entire real line $(-\infty, \infty)$. The error made in doing so is expected to be of order $\exp(-\text{constant}/g^2)$, and therefore negligible compared with powers of g , as $g \rightarrow 0$. A typical example is given by

$$\int_{-\pi}^{\pi} dx e^{-x^2/g^2} = \int_{-\infty}^{\infty} dx e^{-x^2/g^2} + O(e^{-\pi^2/g^2}). \tag{5.131}$$

(b) For a $U(1)$ gauge theory show that (5.130) leads to a Faddeev–Popov factor that is independent of U ,

$$\Delta(U) = \text{constant} \times \det(\square), \quad \square_{xy} = \partial'_\mu \partial_\mu \bar{\delta}_{xy}, \tag{5.132}$$

with the constant independent of A_μ .

(ii) *Weak-coupling expansion in compact QED*

We consider first the bosonic theory given by the action

$$S(U) = -\frac{1}{2g^2} \sum_{x\mu\nu} (1 - U_{\mu\nu x}) \tag{5.133}$$

and use (5.130) for gauge fixing. The bare vertex functions $-V$ are given by

$$S_A + S_{\text{gf}} = - \sum_n \frac{1}{n!} \sum_{x_1 \cdots x_n} V_{\mu_1 \cdots \mu_n}^{x_1 \cdots x_n} A_{\mu_1 x_1} \cdots A_{\mu_n x_n}. \tag{5.134}$$

(a) Show that, in momentum space, for even $n \geq 2$ (by convention the momentum-conserving periodic delta function is omitted in the definition of the Fourier transform of $V_{\mu_1 \dots \mu_n}^{x_1 \dots x_n}$),

$$V_{\mu_1 \dots \mu_n}(k_1 \dots k_n) = -\frac{1}{2}(g^2)^{n/2-1} \sum_{\alpha\beta} T_{\mu_1}^{\alpha\beta}(k_1) \dots T_{\mu_n}^{\alpha\beta}(k_n) - \delta_{n,2} \frac{1}{\xi} K_{\mu_1}(k_1) K_{\mu_2}(k_2), \quad (5.135)$$

where

$$K_\mu(k) = \frac{1}{i}(e^{ik_\mu} - 1), \quad K_\mu^*(k) = -K_\mu(-k), \quad (5.136)$$

$$T_\mu^{\alpha\beta}(k) = K_\alpha^*(k) \delta_{\beta\mu} - K_\beta^*(k) \delta_{\alpha\mu}. \quad (5.137)$$

(b) Show that the photon propagator $D_{\mu\nu}(k)$ is given by

$$D_{\mu\nu}(k) = \left(\delta_{\mu\nu} - \frac{K_\mu(k) K_\nu^*(k)}{|K(k)|^2} \right) \frac{1}{|K(k)|^2} + \xi \frac{K_\mu(k) K_\nu^*(k)}{|K(k)|^4}. \quad (5.138)$$

The Feynman gauge corresponds to $\xi = 1$.

(c) Derive (5.19), for arbitrary ξ .